Supporting Information

Freeze-resistant multi-functional organohydrogel reinforced with bi-metallic MOFs for advanced strain sensors and flexible communication devices

Shafia Anum, Al Nimra, Luqman Ali Shah*

Polymer Laboratory, National Centre of Excellence in Physical Chemistry, University of Peshawar, Peshawar 25120 Pakistan

*Corresponding author

Email: luqman_alisha@uop.edu.pk

Tel: (9291)9216766

Synthesis of ZnZr Bi-Metallic MOFs

This work used the hydrothermal method to prepare a Bi-Metallic metal-organic framework, which is referred to as Bi-MOFs. The organic linker used was benzene tricarboxylic acid (BTC), also referred to as trimesic acid (Tma), and the precursors were Zn $(NO_3)_2.6H_2O$ and $ZrOCl_2.8H_2O$. The standard method involved dissolving 0.595 g of Zn $(NO_3)_2.6H_2O$ and 0.676 g of $ZrOCl_2.8H_2O$ in 51 ml of a 1:1:1 mixture of water, DMF, and ethanol. 0.8 g of Tma was also added and stirred for half an hour at room temperature. After that, the uniform mixture was put into a 100 ml autoclave. The autoclave was kept in an oven set at 120 °C for 24 hrs. White crystals were eventually extracted, filtered, and repeatedly cleaned with ethanol. After being dried at 80 °C in an oven, the resultant product was put aside for further analysis.

Structure of ZnZr Bi-MOFs

Supporting Information

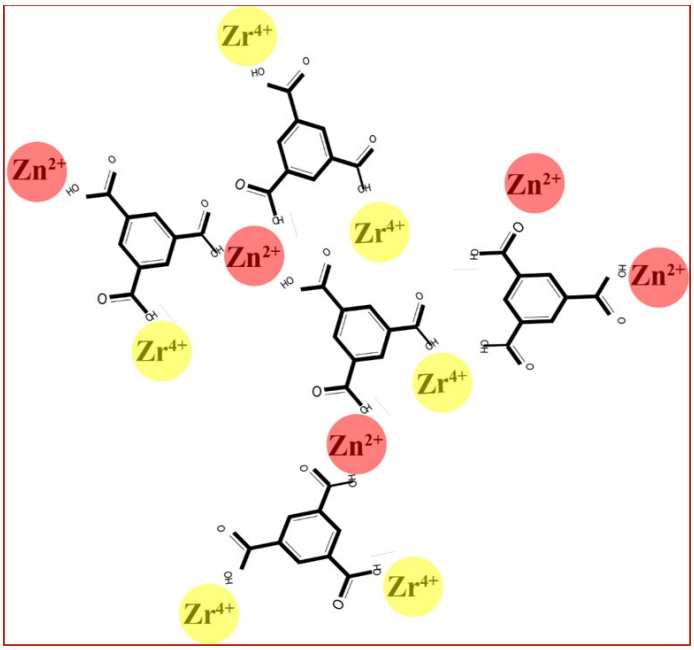

Characterization of ZnZr Bi-MOFs

The ZnZr Bi-MOFs' functional groups were identified using Fourier-transformed infrared spectroscopy (FTIR) with the Bruker Corp Vertex-70V; the corresponding spectra are shown in Figure S1. A wide peak that shows the O-H stretching vibration of methanol, the carboxylic group of BTC, and the water molecule can be seen at 3500-3604 cm^{-1}. Deformation vibrations are also seen at 734 cm^{-1}. These bands imply that the water molecule is essential to the preparation of Bi-MOFs in addition to acting as a solvent [1]. Furthermore, the asymmetric and symmetric vibrations of the linked carboxylate groups accounted for the bands seen at 1590–1668 cm^{-1} and 1450–1382 cm^{-1}, respectively. This demonstrates that ZnZr Bi-MOFs were successfully prepared. The band at 661 cm^{-1} and 536-443 cm^{-1}, which corresponds to the distinctive vibration of the metal ion (Zr-O_2 and Zn-O), further supports this interpretation [2, 3].

Supporting Information

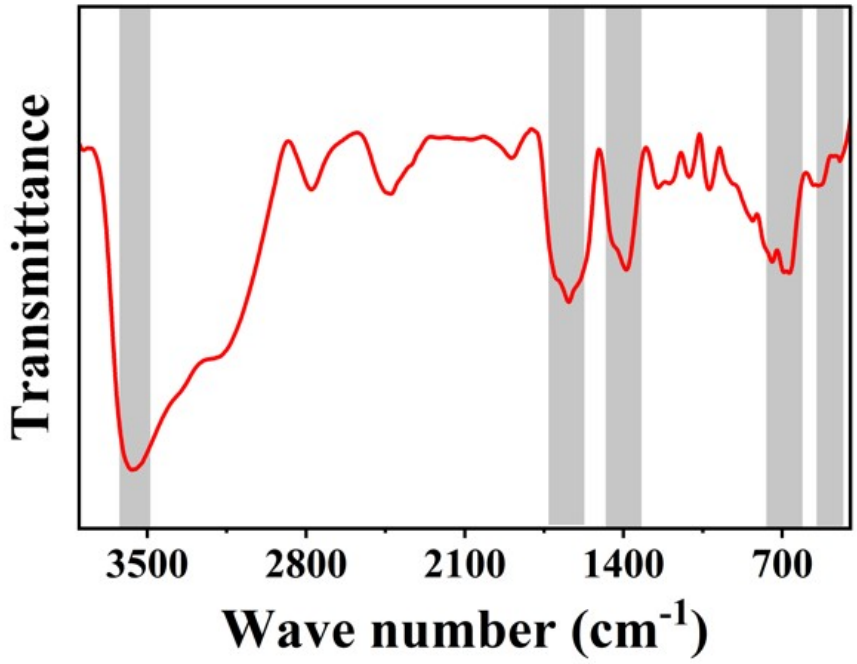

Figure S1: FTIR spectrum of synthesized ZnZr Bi-MOFs.

For finding out more about the crystallographic analysis, the prepared ZnZr Bi-MOFs were subjected to Malvern Panalytical Ltd. EMPYREAN Cu Tube, 40kV, 30mA mode Gonio for X-ray Diffraction (XRD) analysis, as shown in Figure S2. The XRD pattern of the synthesized ZnZr Bi-MOFs exhibits a series of sharp reflections in the low-angle region ($2\theta < 20°$), which is characteristic of highly ordered porous metal–organic frameworks. The intense diffraction peak around 8–9° and the subsequent minor peaks up to 20° confirm the crystalline nature of the framework and indicate the successful formation of a ZnZr coordinated MOF structure. The absence of any noticeable peaks corresponding to ZnO (31.7°, 34.4°, 36.2°) or ZrO_2 (30–35°) demonstrates that no metal oxide impurities were formed during synthesis. Moreover, the low intensity at higher diffraction angles (> 25°) indicates the preservation of a highly porous structure. These observations collectively confirm the formation of a crystalline ZnZr Bi-MOFs with good phase purity and without oxide by-products [4, 5].

Supporting Information

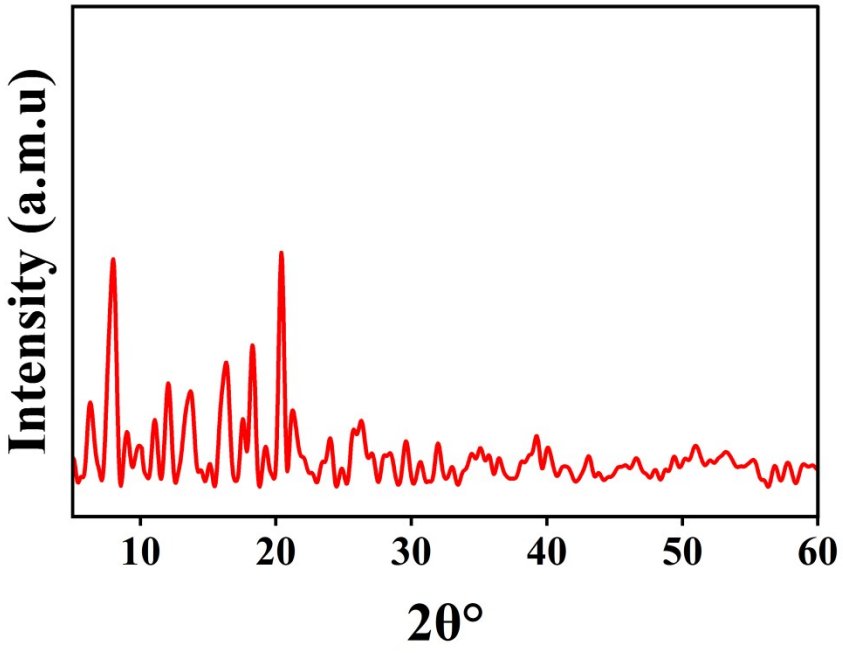

Figure S2: XRD pattern of ZnZr Bimetallic MOFs.

Energy-dispersive X-ray spectroscopy (EDX) analysis was carried out at 20 kV using a JEOL IT100LA instrument to determine the elemental composition and confirm the successful incorporation of Zn and Zr metals within the Bi-Metallic MOF framework. The EDX spectrum (Figure S3a-b) clearly shows distinct signals and elemental ratios corresponding to Zn and Zr, along with the peaks of C and O originating from the organic linkers and framework structure. The uniform distribution of Zn and Zr throughout the sample, as demonstrated by the EDX elemental mapping (Figure S3c), indicates the homogeneous incorporation of both metal species into the MOF lattice without noticeable segregation or phase separation. Importantly, no additional peaks corresponding to other metallic impurities were detected, confirming the purity of the synthesized material.

Supporting Information

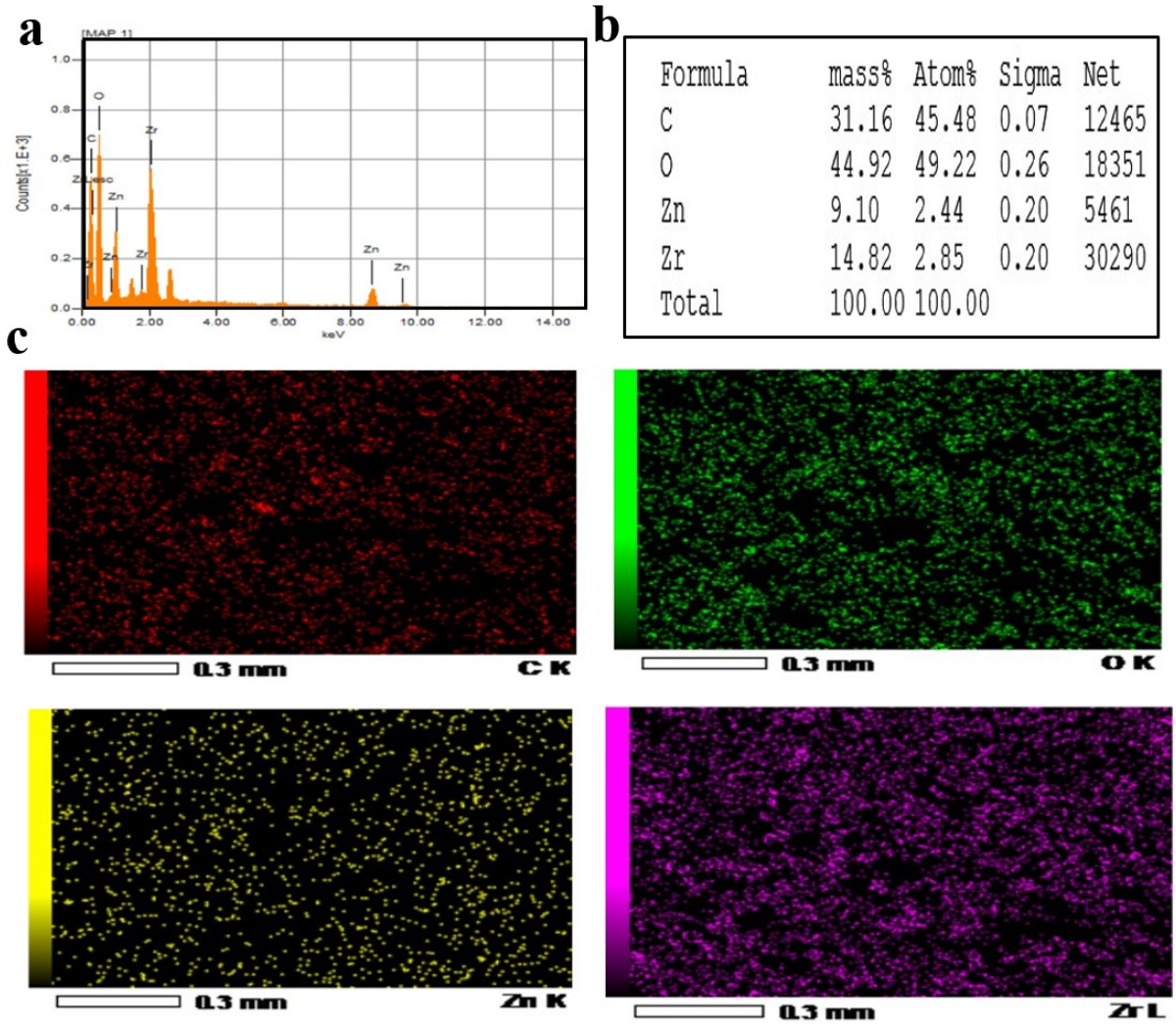

Figure S3: Illustration of MOFs (a) EDX graph, (b) Percentage map of the EDX, (c) Photographs of different elements.

Supporting Information

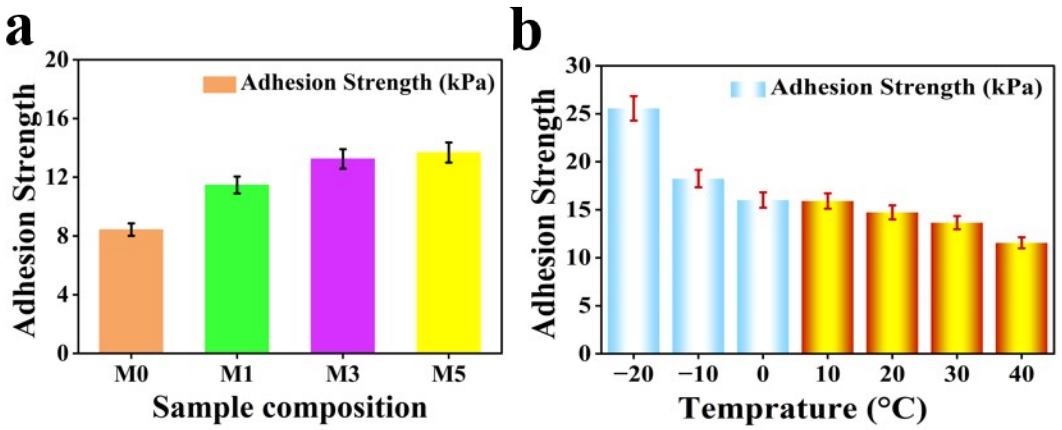

Figure S4. (a) Adhesion Strength of different samples, (b), and M5 temperature-dependent behavior.

Table S1 Comparison of the principal performance outcomes of this research with those reported in recent similar studies.

Organohydrogel Samples	**Stretchability (%)**	**Tensile Strength (MPa)**	**Conductivity (S/m)**	**Sensitivity (GF)**	**Response/ recovery time (ms)**	**References**
PANI/P(AAm-co-AAc) Organohydrogel	628	0.14	0.27	3.88	731/664	[6]
PMTAG Organohydrogel	1740	0.184	0.0224	3.86	350/320	[7]
MOF/PAA-SN Organohydrogel	1995	0.2	-	2.4	577/578	[8]
P(AAm-co-GG)@AMH Organohydrogel	717	0.116	0.468	9.34	47/154	[9]
GW-SF Organohydrogel	2227	20.78	5.7	0.41	-	[10]
(CNCs-g-(W-PAm/PMMA-O) Organohydrogel	2100	0.6	0.29	12	120/100	[11]

PAM/SA/TOCN Organohydrogel	681	1.04	1.25	2.1	-	[12]
PAAN/Gly Organohydrogel	2150	1.35	2.23	8.43	160/200	[13]
ANF-PVA Organohydrogel	484	2.25	13.1	1.99	-	[14]
P (Am/MMA)@ ZnZr Bi-MOFs Organohydrogel	2500	0.37	0.35	7.58	110/90	**Current work**

References

1. Khan, M., et al., *Bimetallic-MOF Tunable Conductive Hydrogels to Unleash High Stretchability and Sensitivity for Highly Responsive Flexible Sensors and Artificial Skin Applications.* ACS Applied Polymer Materials, 2024. **6**(12): p. 7288-7300.
2. Thongam, D.D., J. Gupta, and N.K. Sahu, *Effect of induced defects on the properties of ZnO nanocrystals: surfactant role and spectroscopic analysis.* SN Applied Sciences, 2019. **1**(9): p. 1030.
3. Lestari, W.W., et al., *Post-Synthesis Modification of Zirconium (IV)-BTC Based MOF with Palladium Nanoparticles as Catalyst in the Hydrogenation Reaction of Citronellal.* Journal of Inorganic and Organometallic Polymers and Materials, 2024. **34**(3): p. 1337-1349.
4. Zhang, X., et al., *Green photocatalysis of organic pollutants by bimetallic Zn-Zr metal-organic framework catalyst.* Frontiers in Chemistry, 2022. **10**: p. 918941.
5. Gupta, G., et al., *Removal of organic dyes from aqueous solution using a novel pyrene appended Zn (II)-based metal–organic framework and its photocatalytic properties.* Dalton Transactions, 2024. **53**(37): p. 15732-15741.

Supporting Information

6. Chen, G., et al., *Flexible artificial tactility with excellent robustness and temperature tolerance based on organohydrogel sensor array for robot motion detection and object shape recognition.* Advanced Materials, 2024. **36**(45): p. 2408193.
7. Zou, Y., et al., *Ultra-Stretchable Composite Organohydrogels Polymerized Based on MXene@ Tannic Acid-Ag Autocatalytic System for Highly Sensitive Wearable Sensors.* Small, 2024. **20**(47): p. 2404435.
8. Li, Y., et al., *A metal–organic framework enhanced single network organohydrogel with superior low-temperature adaptability and UV-blocking capability towards human-motion sensing.* Journal of Materials Chemistry C, 2025. **13**(2): p. 724-734.
9. Khan, A.A., et al., *Flexible organohydrogel epidermal sensors with superior anti-freezing and strain sensitivity for extreme environmental applications.* Sustainable Materials and Technologies, 2025: p. e01474.
10. Dong, X., et al., *An organo-hydrogel with extreme mechanical performance and tolerance beyond skin.* Materials Today, 2024. **72**: p. 25-35.
11. Sher, M., et al., *Hybrid strengthening of cellulose nanocrystal-based solvent co-cross linked flexible organohydrogels with fast self-healing, diverse adhesive nature, and anti-freezing behavior for advanced human health monitoring.* Journal of Materials Chemistry B, 2025. **13**(15): p. 4612-4629.
12. Cheng, Y., et al., *Nanocellulose-enhanced organohydrogel with high-strength, conductivity, and anti-freezing properties for wearable strain sensors.* Carbohydrate Polymers, 2022. **277**: p. 118872.
13. Su, G., et al., *Soft yet tough: a mechanically and functionally tissue-like organohydrogel for sensitive soft electronics.* Chemistry of Materials, 2022. **34**(3): p. 1392-1402.

Supporting Information

14. Lyu, J., et al., *Mechanically strong, freeze-resistant, and ionically conductive organohydrogels for flexible strain sensors and batteries.* Advanced Science, 2023. **10**(9): p. 2206591.